



LJMU Research Online

Klare, H, Neudörfl, JM, Brandt, SD, Mischler, E, Meier-Giebing, S, Deluweit, K, Westphal, F and Laussmann, T

Analysis of six “neuro-enhancing” phenidate analogs

<http://researchonline.ljmu.ac.uk/id/eprint/5244/>

Article

Citation (please note it is advisable to refer to the publisher’s version if you intend to cite from this work)

Klare, H, Neudörfl, JM, Brandt, SD, Mischler, E, Meier-Giebing, S, Deluweit, K, Westphal, F and Laussmann, T (2017) Analysis of six “neuro-enhancing” phenidate analogs. Drug Testing and Analysis. ISSN 1942-7611

LJMU has developed **LJMU Research Online** for users to access the research output of the University more effectively. Copyright © and Moral Rights for the papers on this site are retained by the individual authors and/or other copyright owners. Users may download and/or print one copy of any article(s) in LJMU Research Online to facilitate their private study or for non-commercial research. You may not engage in further distribution of the material or use it for any profit-making activities or any commercial gain.

The version presented here may differ from the published version or from the version of the record. Please see the repository URL above for details on accessing the published version and note that access may require a subscription.

For more information please contact researchonline@ljmu.ac.uk

<http://researchonline.ljmu.ac.uk/>

Analysis of six “neuro-enhancing” phenidate analogs

Helge Klare,^a Jörg M. Neudörfl,^b Simon D. Brandt,^c Elisabeth Mischler,^a Sigrid Meier-Giebing,^a Kathrin Deluweit,^a Folker Westphal,^d Tim Laussmann^{a,*}

^a Central Customs Authority, Centre of Education and Science, 50765 Cologne, Germany

^b University of Cologne, Department of Chemistry, Organic Chemistry, 50939 Cologne, Germany

^c School of Pharmacy and Biomolecular Sciences, Liverpool John Moores University, Liverpool, L3 3AF, UK

^d State Bureau of Criminal Investigation Schleswig-Holstein, Section Narcotics/Toxicology, D-24116, Kiel, Germany

* Correspondence to: Tim Laussmann, Central Customs Authority, Centre of Education and Science, 50765 Cologne, Germany. E-Mail: tim.laussmann@bwz.bund.de

This article has been accepted for publication and undergone full peer review but has not been through the copyediting, typesetting, pagination and proofreading process which may lead to differences between this version and the Version of Record. Please cite this article as doi: 10.1002/dta.2161

Abstract

Six collected phenidates, i.e. 4-methylmethylphenidate, 3,4-dichloromethylphenidate, ethylphenidate, 3,4-dichloroethylphenidate, ethylnaphthidate and *N*-benzyl-ethylphenidate were fully characterized by means of X-ray, NMR, GC-MS, ESI-MS², ATR-FT-IR and GC solid-state IR analysis. Crystallography revealed the exclusive presence of the *threo*-configuration. Steric crowding induced by *N*-benzyl substitution at the piperidine moiety prompted an adoption of an unexpected axial positioning of substituents on the piperidine moiety in the crystal state as opposed to the exclusive equatorial positioning encountered in *N*-unsubstituted phenidate analogs. Gas phase computations of the relative lowest energy conformers confirm that the axial positioning appears to be favored over the equatorial positioning, however in solution equatorial positioning is predominant according to NOE experiments. All samples, mainly originating from China, had a good to very good degree of purity indicative of their professional chemical synthesis. Routine analysis of these drugs by GC-MS revealed thermal decomposition of phenidate analogs in the injection port and/or on column to 2-aryl-ethyl-acetates and 2,3,4,5-tetrahydropyridines. The decomposition pathway was suggested to proceed *via* a 6-membered transition state which was supported by DFT-computations. Fragmentation pathways of decomposition products as well as the corresponding EI mass spectra are provided. The thermal instability might thus render smoking or “vaping” of these drugs a less effective route of administration. The analytical fingerprints of six structurally diverse phenidate analogs provide a helpful reference to forensic chemists in charge of identifying new psychoactive substances.

Running title: Analytical characterization of six phenidate analogs

Keywords: Phenidates; forensic; computation; smart drugs; chemical analysis; legal high; NPS

Introduction

New psychoactive substances (NPS) are drugs that are chemically altered relatives of known controlled drugs. From a European perspective, the definition of NPS includes substances that are not listed in any of the schedules to the 1961 United Nations Single Convention on Narcotic Drugs as well as the 1971 United Nations Convention on Psychotropic Substances and which may pose a comparable threat to public health as the substances listed in these schedules.^[1,2] As many of these compounds are not yet listed, they are euphemistically advertised as “legal highs”, “bath salts” or “research chemicals” in many countries. Distribution and supply of NPS is mostly facilitated through online shops and high street retailers and their availability has increased drastically in recent years, with a sevenfold increase in reported seizures in the EU between 2008 and 2013. The European Monitoring Centre for Drugs and Drug Addiction (EMCDDA), through the EU Early Warning System, is currently monitoring more than 560 substances.^[3] In 2015 alone, the EU early warning system reported 98 new compounds with synthetic ring substituted cathinones, synthetic cannabinoids and phenylethylamines representing the major contributions.^[4,5] Seizures of the Central Customs Authority in Germany are in accordance with these numbers, with cathinones (42 %), cannabinoids (38 %) and phenethylamines (17 %) accounting for the majority of all NPS cases dealt with in the years 2012-2015. Strikingly, these data reflect the general trend in an ever faster developing drug market: While in 2012 a total of 13 different (at that time) legal NPS were registered in our laboratories, this number doubled to 26 in 2015 and is likely to further increase in 2016 (Figure 1).

As a relatively new class of phenethylamines, a number of phenidate derivatives are available on the NPS drug market. Phenidates are chemical analogs of methylphenidate (**1**) which is well known as the prescription drug Ritalin[®]. Methylphenidate is clinically used in the

treatment of attention deficit hyperactivity disorder (ADHD). It acts as a reuptake inhibitor at the dopamine transporter (DAT) ($K_i = 640$ nM for (-)-cocaine and 390 nM for *D-threo*-methylphenidate), and also acts as a blocker of norepinephrine uptake. However, unlike cocaine, nearly no activity at the serotonin transporter (SERT) was reported.^[6-8] Methylphenidate increases central nervous system activity and effects at lower doses include improved cognition, heightened alertness and reduced fatigue whereas higher doses can induce euphoria.^[9-12] On these grounds methylphenidate has been abused as a recreational drug since the 1960s and more recently as a “neuroenhancing” “smart drug”.^[12,13] Possible side effects related to methylphenidate overdoses include tachycardia, hallucinations and psychosis.^[11,13] Since methylphenidate is a widely regulated pharmaceutical, structurally diverse and often more potent NPS of the phenidate class have entered the drug market.^[14,15] Molecular structures and the respective activities at the DAT have been reported for many of these compounds in the scientific literature, thus making the targeted synthesis of potent phenidate analogs for the drug market likely.^[16] Phenidates were also recently seized by German authorities, such as 4-methylmethylphenidate (**2**), 3,4-dichloromethylphenidate (**3**), ethylphenidate (**4**), 3,4-dichloroethylphenidate (**5**), and *N*-benzyl-ethylphenidate (**7**), while the related ethylnaphthidate (**6**) is sold online in the United Kingdom (Figure 2). Little is known about the pharmacology and hazards of phenidate analogs despite their structural similarity.^[11,12,16-18] However, ethylphenidate (**4**) has been linked to a number of deaths^[19-23] and concerns have been expressed about ethylphenidate injection in drug users.^[21,22] It has also been long recognized that ethylphenidate is formed *in vivo* following co-administration of methylphenidate with alcohol.^[25,26]

The reaction of governments in the European Union to the challenge posed by NPS can be broadly differentiated into three legal response types. These may consist of a) the application of existing laws designed for consumer- or health-protection and pharmaceutical legislation;

b) amending of drug laws by e. g. introducing group definitions of controlled substances; c) innovative approaches that e. g. define a substance by its psychoactive effect rather than its chemical structure.^[27] Procedure a) can be difficult to implement and pharmaceutical legislation in e.g. Germany is not applicable to “substances that [...] are only consumed to intoxicate while being detrimental to health” according to a recent ruling by the European Court of Justice (ECJ).^[28] Thus, Germany has recently introduced chemical group definitions b) like other countries in the EU. The corresponding new law defines new psychoactive substances as substances that are covered by the chemical compound groups defined in the annex to that law.^[29]

Authorities and forensic chemists need to reliably elucidate the type of NPS in question. While this is feasible by combining routine analytical methods provided that the NPS are listed in existing databases, difficulties arise when a NPS is not well documented or unknown. To assist efforts in the reliable structural elucidation of NPS, this study presents an extensive characterization of newly emerging phenidate analogs **2-7**.

Experimental

Chemicals

Chemicals were purchased from Sigma-Aldrich (Steinheim, Germany) and used as purchased without further purification. CDCl_3 and D_2O were obtained from Sigma-Aldrich (Steinheim, Germany) and Deutero GmbH (Kastellaun, Germany). All solvents and reagents used were of analytical grade. Phenidates **2**, **3**, **4**, **5** and **7** were parts of confiscations by German authorities whereas naphthidate **6** was obtained from a test purchase.

Sample preparation

For the analysis of the compounds **2** to **7** by gas chromatography mass spectrometry (GC-MS) approximately 1 mg of the salts were dissolved in 1 mL ethanol. For the analysis of the compounds **2** to **7** by quadrupole time-of-flight electrospray ionization tandem mass spectrometry (QTOF-ESI-MS/MS) approximately 1 mg of the hydrochloride salts were dissolved in 1 mL ethanol. Furthermore, 40 μL of this solution were diluted with 1 mL of $\text{H}_2\text{O}/\text{MeCN}/\text{FA}$ (100:100:0.1, *v/v*) in a standard vial. For the analysis of the compounds **2** to **7** by nuclear magnetic resonance spectroscopy (NMR) ca. 20 mg of the respective salts were dissolved in 0.6 mL CDCl_3 (**2**, **4-7**) or 0.75 mL CDCl_3 + 40 μL MeOD (**3**). Infrared spectra (IR) of all compounds were recorded as their hydrochloride salts. For the analysis of the compounds **2** to **7** by infrared spectroscopy as their free bases, a small portion of the hydrochloride salts (ca. 10 mg) were dissolved in demineralized water and then alkalized with a few drops of aqueous sodium hydroxide solution. Diethyl ether was added to the aqueous solution. The organic phase was transferred directly to the ATR crystal yielding the free base after evaporation of diethyl ether. For analysis by X-ray diffraction, the crystals obtained from the confiscated samples (as their hydrochloride salts) had sufficient quality to

be directly subjected to X-ray crystallography in the cases of **2**, **4** and **7**. The compounds **3**, **5** and **6** had to be recrystallized from MeOH/EtOAc.

Gas chromatography mass spectrometry (GC-MS) (routine method of analysis)

Electron ionization (EI) mass spectra were obtained from a DSQ II quadrupole mass spectrometer (Thermo Scientific, Dreieich, Germany) coupled to a gas chromatograph (Focus GC, Thermo Scientific, Dreieich, Germany) with an auto sampler AS 3000 (Thermo Scientific, Dreieich, Germany). Samples (1 μL) were introduced *via* the gas chromatograph with split injection 1:100 using a fused silica capillary column Zebron 2B-5 (30 m \times 0.25 mm, film thickness 0.25 μm) (Phenomenex, Aschaffenburg, Germany). The temperature program started with an initial temperature of 50 $^{\circ}\text{C}$, held for 2 min, followed by a ramp to 240 $^{\circ}\text{C}$ with 16 $^{\circ}\text{C}/\text{min}$ and held for 1 min. The final temperature was 300 $^{\circ}\text{C}$ using a 30 $^{\circ}\text{C}/\text{min}$ temperature ramp and held for 5 min, thus resulting in a total run time of 22 min. The injector temperature was 260 $^{\circ}\text{C}$. The transfer line temperature was maintained at 280 $^{\circ}\text{C}$. The carrier gas (helium) was set at a constant flow rate of 1.8 mL/min. The electron ionization (EI) energy was 70 eV with an emission current of 100 μA . The scan time was 0.36 s and the scan range was m/z 40-550. The ion source temperature was maintained at 250 $^{\circ}\text{C}$.

GC-MS (modified protocol)

Chromatograms and EI mass spectra were obtained with a GCMS-QP2010SE GC-MS (Shimadzu, Duisburg, Germany) with a GC 2010 plus auto sampler (Shimadzu, Duisburg, Germany). Samples (0.5 μL) were introduced *via* the gas chromatograph with split injection 1:100. For separation, a fused silica capillary column Optima-1 MS Accent (30 m \times 0.25 mm, film thickness 0.25 μm) (Macherey-Nagel, Düren, Germany) was employed. The temperature program started with an initial temperature of 50 $^{\circ}\text{C}$, held for 2 min, followed by a ramp to

230 °C with 7 °C/min, and held for 2 min. The final temperature was 300 °C, reached with 35 °C/min and held for 5 min, thus resulting in a total run time of 36 min. The injector temperature was 260 °C. The transfer line temperature was maintained at 280 °C. The carrier gas was helium in constant flow mode at a flow rate of 1.8 mL/min. The electron ionization (EI) energy was 70 eV with an emission current of 100 µA. The scan time was 0.36 s and the scan range was m/z 40-550. The ion source temperature was maintained at 250 °C.

Quadrupole time-of-flight electrospray ionization tandem mass spectrometry (QTOF-ESI-MS/MS)

The employed mass spectrometer was a Bruker micrOTOF-Q III (Bruker, Bremen, Germany) coupled with an electrospray ionization source operated in positive ion mode. Sodium formate was used as calibration standard and Bruker DataAnalysis 4.2 SR1 Workstation Software was used for data analysis. Samples were introduced *via* continuous direct infusion with a syringe-pump set to 180 µL/h and a drying gas flow of 4 L N₂/min. Drying gas temperature was set to 180 °C, nebulizer pressure to 0.3 bar and capillary voltage to 2500 V. Flow injection analysis (FIA) was employed to optimize the collision energy (CE) for each multiple reaction monitoring (MRM) transition.

Nuclear magnetic resonance spectroscopy (NMR)

NMR spectra for compounds **2-6** were recorded using a Bruker UltraShield (7.05 Tesla, 300 MHz) Fourier 300 spectrometer (Bruker, Coventry, UK) equipped with a dual ¹H/¹³C probe (5 mm) with 2H lock and fitted with a z gradient coil at 298 K. The NMR spectrum for compound **7** was recorded at the NMR spectrometry facility of the Institute for Organic Chemistry of the University of Cologne. The one- and two-dimensional NMR measurements (¹H-NMR, ¹³C-DEPT, ¹H/¹H-COSY, ¹H/¹³C-HSQC, ¹H/¹³C-HMBC and ¹H/¹H-NOESY)

were performed with a Bruker Avance II+ 600 NMR spectrometer (resonance frequency for ^1H 600.20 MHz) with a H,P,X TBI z-Grad probe at 298 K and internal chemical shift references were based on residual solvent peaks. Suggested assignments were aided by 1-D and 2-D experiments and internal chemical shift references were based on residual solvent peaks.

Infrared spectroscopy (IR)

The spectrometer used was a Bruker Alpha FT-IR (Bruker, Ettlingen, Germany) equipped with a diamond platinum ATR crystal. The wavelength resolution was set to 4 cm^{-1} . IR spectra were collected in a range of $400\text{--}4000\text{ cm}^{-1}$ with 20 scans per spectrum.

X-ray diffraction

The diffractometer employed was a Bruker D8 Venture with Kappa-goniometer and a Cu-Microfocus X-ray source (Bruker, Karlsruhe, Germany). Crystallographic data have been deposited with the Cambridge Crystallographic Data center. These data can be obtained online free of charge from the Cambridge Crystallographic Data Centre (CCDC).^[30] CCDC 1520751 (2), CCDC 1520753 (3), CCDC 1520750 (4), CCDC 1520752 (5), CCDC 1520755 (6) and CCDC 1520749 (7) contain the supplementary crystallographic data for this compound.

Computational details

All theoretical calculations were performed with the program package TURBOMOLE-7.0.2 and density functional theory (DFT).^[31] The employed density functional was the GGA BP86-functional developed by Becke and Perdew, combined with the contracted def2-SVP or def2-TZVP basis sets by Ahlrich *et al.*^[32,33] as specified. On transition states, subsequent single point calculations employing the B3LYP-functional were conducted.^[34] For some

calculations the dispersion correction DFT-D3(BJ) was used as specified.^[35,36] The multipole accelerated resolution of identity approximation for two electron integral evaluation was used. All stationary points were fully optimized and confirmed by separate analytical frequency calculations. Transition structures were optimized with quasi-Newton–Raphson methods by using the Powell update algorithm for hessian matrix approximation (subsequent analytical frequency calculation). Absolute energies were zero-point corrected with the vibrational information received from harmonic analytical frequency calculations. Coordinates of transition structures and stationary points can be found within the Supporting Information.

Results and discussion

X-ray diffraction

Crystal structure analysis revealed that all six phenidate analogs were hydrochloride salts. Crystal structures of **2** and **3** have been previously published by Deutsch *et al.* and are in agreement with our own measurements.^[37] The crystal structures of the phenidate analogs, depicted as the (*R,R*)-enantiomers, are shown in Figure 3, although all measured crystals consisted of racemic material as evident from their point groups. The defining dihedral angles and distances for all compounds are summarized in Table 1. For all measured samples the (\pm)-*threo*-configuration of the phenidate analogs was confirmed. All (\pm)-*threo*-phenidate analogs without substituents on nitrogen have closely related conformations with the piperidine ring in the chair conformation and the ring-substituent in equatorial position. The conformation of the carbonyl oxygen O1 is similar for compounds **3-6** with close proximity between O1 and the ammonium group (N1-O1: 3.21 – 3.46 Å), constituting to a weak intramolecular hydrogen bond. However, in 4-methyl-methylphenidate **2** and *N*-benzyl-

ethylphenidate **7** the ester-group is rotated by approximately 180°, with the oxygen O2 closer to the ammonium hydrogen. Since there are no further intermolecular strong or medium hydrogen bonds involving O1 in the crystal structure of **2** or **7**, loss of the intramolecular hydrogen bond between O1 and N1 is compensated by a shorter N1-O2 (3.02 - 3.14 Å) hydrogen bond. Furthermore for all compounds **2-7** the terminal ethyl(methyl) group as seen along the O2-C1 axis eclipses the carbonyl oxygens in *anti*-conformation as expected.

In contrast to the crystal structures of **2-6**, *N*-benzyl-ethylphenidate **7** exhibits a markedly different conformation. Most strikingly, substituents on the piperidine ring are in axial positions. Furthermore, the ethyl-moiety as seen along the O2-CH₂ axis is in a *gauche*-conformation. Both, axial position of substituents and the *gauche* conformation are potentially sterically more demanding and thus energetically disfavored. A conformational analysis was conducted by density functional theory (DFT) computations employing the program package Turbomole 7.0.2. It was determined whether the unusual conformation of **7** in the crystalline state might also represent the energetically most favored candidate. According to computational analysis, the axial positioning of substituents found in the crystal structure is the least favored one in the gas phase (*ax-7-1* $E_{\text{rel}} = 2.1 \text{ kcal mol}^{-1}$, cf. Supporting Information Figure S 66) of all computed structures. This can indeed be attributed to steric repulsion between the *N*-benzylic group and the ester moiety as well as the disfavored ethyl group *gauche*-conformation of the latter. However, a related axial positioning *ax-7-2* with an *anti*-conformation of the ethyl-moiety and a rotated ester moiety (C1-C2 axis) decreases steric repulsion and represents the lowest energy conformation. The lowest energy conformation with substituents in equatorial positions is thermodynamically slightly less favorable ($E_{\text{rel}} = 0.7 \text{ kcal mol}^{-1}$), possibly because of steric repulsion between the *N*-benzylic moiety and the ester moiety. Moreover, intermolecular hydrogen bonding might also contribute to stabilizing the observed axial conformation among long-range forces in the

crystal although this has not been accounted for by the simplified computational model. Similar to the crystal structures of **3**, **4**, **5** and **6**, the carbonyl oxygen is rotated to closer proximity to the ammonium group in *ax-7-2*, constituting a weak hydrogen bond. The relatively small energetic difference between the axial and equatorial conformation in **7** (in gas phase) and its high steric bulk might help to explain the divergent pharmacological profile of some *N*-benzyl-substituted phenidates that have been shown to display SERT binding ($[^3\text{H}]\text{CIT}$) comparable to (-)-cocaine.^[38]

NMR

To the best of our knowledge NMR data of the phenidate analogs investigated in this publication have only been published for phenidates **3** and **4**.^[39,40] For all compounds the following spectra were recorded: ^1H -NMR, ^{13}C -DEPT, $^1\text{H}/^1\text{H}$ -COSY, $^1\text{H}/^{13}\text{C}$ -HSQC, $^1\text{H}/^{13}\text{C}$ -HMBC. For the only *N*-benzyl-substituted ethylphenidate **7** an additional $^1\text{H}/^1\text{H}$ -NOESY correlation spectrum was recorded. All compounds were soluble in CDCl_3 as their salts except for 3,4-dichloromethylphenidate **3** which was soluble (20-30 mg in 0.75 mL deuterated solvent) only after addition of 40 μL MeOD. Generally, from ^1H NMR a relatively high purity of all investigated compounds was evident, with only minor traces of impurities indicating a high degree of professionalism in the manufacture of these drugs. The ^{13}C and ^1H NMR assignments of all compounds are summarized in Table 2, the corresponding spectra can be found in the Supporting Information (Figures S1-13). The ^1H NMR spectrum of 3,4-dichlorethylphenidate **5** with assignments is depicted in Figure 4.

For all compounds, the signals for NH-protons were in the region of 8.38-10.36 ppm, except for *N*-benzyl-ethylphenidate **7** where the NH-proton was shifted further downfield to 12.48 ppm. Resonance of the α -proton H-2 occurred as a doublet at 4.26-4.38 ppm for compounds **2**

to **6** with similar coupling constants [$^3J_{\text{H2-H3}} \approx 10$ Hz] where they could be determined. For compound **7** resonance of H-2 was shifted downfield to 5.02 ppm with a lower coupling constant [$^3J_{\text{H2-H3}} = 8.3$ Hz]. Moreover, shifts for the CH-proton H-2' alpha to nitrogen were typically recorded at 3.65-3.97 ppm. The diastereotopic protons H-6'' α /H-6'' β were significantly separated for **2-6** and recorded around 3.53-3.87 ppm and 2.86-3.04 ppm, respectively (for compounds **2, 4, 5** and **6** H-2'' and H-6'' α overlapped in CDCl₃). For **2** and **3**, the singlet of the O-CH₃ group H-1''' was shifted to 3.74 and 3.79 ppm. Spectra were more complex for the ethyl-esters **4-7** with the diastereotopic O-CH₂-CH₃ protons coupling to give a doublet of a quartet at around 4.20-4.34 ppm, which overlapped for all compounds but **7**. Furthermore, for the ethyl-esters **4-7**, the terminal CH₃-group H-2'''' (**4-6**) / H-2''''' (**7**) gave a typical pseudo triplet at 1.13-1.23 ppm for all compounds.

N-Benzyl-ethylphenidate **7** was investigated further by means of a $^1\text{H}/^1\text{H}$ -NOESY experiment. The axial position of substituents on the piperidine ring observed by X-ray crystallographic analysis was of particular interest. A strong nuclear Overhauser effect (NOE) could be observed between the *N*-benzylic proton H-7'' α and the C $_{\alpha}$ -proton H-2 (cf. Figure S 13, Supporting Information). This was an indication for a preferred equatorial position of substituents in solution as these protons would be spaced far apart if substituents were on axial positions of the piperidine ring and thus would not give rise to a NOE contact. Furthermore, if an axial position of substituents was predominant, a NOE between the NH proton and piperidine-proton H-2'' should have been observable, which was not the case.

GC-MS

While all compounds had only minor impurities according to NMR-analysis, the GC data obtained with routine drug analysis were not consistent. The chromatograms of 4-methylmethylphenidate **2**, ethylphenidate **4** and *N*-benzyl-ethylphenidate **7** showed only one major compound peak with minor broadening (**2**: 12.21 min; **4**: 11.89 min; **7**: 15.79 min) as expected. In contrast, the chromatograms of 3,4-dichloromethylphenidate **3**, 3,4-dichloroethylphenidate **5** and ethylnaphthidate **6** showed a strongly broadened major peak (**3**: 12.82 min; **5**: 13.15 min; **6**: 14.62 min) followed by a minor peak (**3**: 13.89 min; **5**: 14.14 min; **6**: 14.96 min) representing the analyte (exemplified with compounds **4** and **6**, Figure 5). The strong peak broadening for ethylnaphthidate **6** (as for compounds **3** and **5**) can be attributed to thermal decomposition in the injection port and/or on column *via* pyrolysis. A 6-membered transition state is proposed for this pyrolysis leading to 2,3,4,5-tetrahydropyridines and 2-aryl-acetates as decomposition products (Figure 6).

This suggestion was consistent with the analysis of the corresponding EI mass spectra. For ethylphenidate **4**, the EI mass spectrum of the major peak (Figure 5 A2, RT: 11.88 min) did not exhibit a signal for the molecular ion and was instead dominated by the base peak at m/z 84. The m/z 84 fragment corresponds to the near quantitative formation of a 2,3,4,5-tetrahydropyridine-1-ium-ion following α -cleavage of the σ -C-C bond adjacent to the piperidine ring in the molecular radical cation (Figure 7, top). Thus, this fragmentation pathway suggested the presence of intact **4** following GC-MS analysis.

With ethylnaphthidate **6**, no such signal was detected at m/z 84 (Figure 5, B2, RT: 14.63 min) but instead, ions at m/z 214, m/z 83 and m/z 141 were detected. This suggested the formation of the molecular radical cations of 2-naphthyl-ethylacetate as well as of 2,3,4,5-tetrahydropyridine and the presence of a cationic fragmentation product of 2-

naphthyl-ethylacetate, respectively. The compounds resulted from pyrolysis of the molecule under GC-conditions. However, for ethylnaphthidate **6** also the fragment at m/z 84 representing the analyte could be detected in the EI mass spectrum of the following minor peak at 14.96 min alongside the thermal decomposition products. Pyrolysis on column was also observed for 3,4-dichloromethylphenidate **3** and 3,4-dichloroethylphenidate **5**. This was consistent with reports related to thermal composition of methylphenidate **1** and compound **3**.^[41,42] While the 2-aryl-acetates and 2,3,4,5-tetrahydropyridine detected in the mass spectra of phenidate analogs could also be the products of a *McLafferty* rearrangement, the peak broadening in the obtained chromatograms seemed to make this unlikely. Peak broadening occurred predominantly for compounds **3**, **5** and **6** with higher molecular weight and subsequently higher retention times. These compounds would have been expected to elute at higher final temperatures when using the standard GC-MS protocol. The exception to this was

N-benzyl-ethylphenidate **7** which, despite having the highest molecular weight of the investigated compounds, only displayed minor peak broadening. This was possibly due to the benzylic “protection group” at the nitrogen atom (cf. Supporting Information, Figure S 29).

This was further supported by computational analysis of the thermal decomposition pathways of a simplified model system where two stepwise and two 6-membered concerted reaction pathways were taken into account. The 6-membered transition states reflected the lowest relative energy. Of these, the transition state **TS-1** leading to 2,3,4,5-tetrahydropyridine is significantly lower in energy than **TS-2** leading to 1,2,3,4-tetrahydropyridine (42.4 kcal mol⁻¹ and 52.0 kcal mol⁻¹ respectively, Figure 8). The thermochemistry of the reactions was computed assuming the conversion of the enol-ester to its ester tautomer (dashed line, Figure 8). Both reactions are endothermic, but, again, the formation of 2,3,4,5-tetrahydropyridine is slightly less so than 1,2,3,4-tetrahydropyridine ($\Delta H = 16.4$ kcal mol⁻¹ and $\Delta H = 17.7$ kcal

mol⁻¹, respectively). This is in good agreement with the observed higher stability of the relatively bulky *N*-benzyl-ethylphenidate **7**: Since no hydrogen atom is available at the nitrogen atom, the decomposition must follow the pathway leading to the 1,2,3,4-tetrahydropyridine product with higher activation barriers and a more stable educt.

To account for these findings, a milder non-standard GC-MS-method was tested for the analysis of 3,4-dichloroethylphenidate **5**. With the standard temperature program the ethyl 2-(3,4-dichlorophenyl)acetate decomposition product was detected nearly exclusively when injecting the HCl salt of **5** (cf. Supporting Information, Figure S 25). With a modified oven-program and a long ramp to 230 °C a relative increase in the amount of 3,4-dichloroethylphenidate **5** could be observed when injecting the HCl salt. Assuming that the HCl salt evaporated at higher temperatures from the GC liner, the free base of **5** was also subjected to the modified GC-protocol which led to an increase in relative peak area for intact **5** along with strong fronting containing the decomposition products. Thus, decomposition of compounds was highly dependent on temperature conditions and the form of the injected substance (salt or base). In GC-CI-MS runs (reagent gas: methane) with **5** only the 2-(3,4-dichloro-phenyl)ethylacetate decomposition product was detected as the protonated molecule $[M + H]^+$ in addition to the typical methane addition products $[M + 29, M + 41]^+$. A similar behavior was observed for the phenidate analogs **3**, **6** and **7**. Furthermore, mass spectra of the intact compounds could also be acquired by direct insertion probe mass spectrometry (CI-MS and DIP-MS for **3**, **5**, **6** and **7**, cf. Supporting Information, Figures S 32-39).

The observed temperature-sensitivity of phenidate analogs might be relevant to forms of consumption of these drugs. For many drugs, vaporizing or smoking is a common route of administration that leads to a very fast onset but shorter duration of effects, thus greatly increasing the addictive potential of these drugs.^[43] There seems to be a debate among

consumers on internet forums whether phenidates are amenable to vaporization, with some claiming strong effects and others observing none. One such report claims:

“I am aware that most of them are somewhat smokable, such as MPA [methylphenidate], but when I tried vaporizing EPH [ethylphenidate] off of foil it just smelt strongly, and I received no discernible effects from the vapour.”^[44]

This statement corresponds well with the fact that ethyl phenylacetate, originating from thermal decomposition of ethylphenidate, is a known food additive and flavoring agent used in perfumery. Thus, temperature-sensitivity of phenidate-derivatives might have implications for particular routes of administration (e.g. smoking or vaporization) in recreational contexts. However, a recent investigation into the experiences reported by ethylphenidate users indicated that the most common route of administration was nasal insufflation whereas vaporization, oral and rectal administrations were less common.^[44]

ESI-MS/MS

The fragments observed in ESI-MS² for ethylphenidate were in agreement with literature data.^[46] Generally, for the phenidate analogs investigated, three distinct product ions with vastly different intensities were observed. The pathways **A-C** are proposed for the collision-induced dissociation of phenidate derivatives following ESI (exemplified with ethylphenidate, Figure 10, Table 3, for all spectra see Supporting Information, Figures S 40-45). Pathway **A** involves the loss of ethylene (-28 Da) from the protonated molecule *via* a concerted 6-membered rearrangement. The resulting product ion at m/z 220 exhibited a very low intensity and could only be observed for ethylester derivatives as only these compounds can rearrange *via* a 6-membered transition state.

Pathway **B** comprises an intramolecular protonation of the ester moiety followed by subsequent loss of ethanol (-46 Da) and carbon monoxide (-28 Da) yielding an arylum ion m/z 174. This signal displayed a lower intensity for compounds **2** and **3** which can be explained by the lower Lewis basicity of the respective methyl esters. Finally, pathway **C** involves a loss of ethyl phenylacetate through rearrangement of the molecule through a mechanism similar to the thermal decomposition of phenidates. This would be expected given the facile rearrangement of the non-protonated phenidates upon heating. However a computation of a protonated model systems reveals a barrier that is slightly higher than that for the unprotonated system ($\text{TS-3} = 57.1 \text{ kcal mol}^{-1}$) and is therefore in agreement with the experiment. The slightly higher barrier also explains the only minor decomposition of phenidate analogs in ESI (drying gas temperature: 180 °C).

IR

IR spectra of all six phenidates **2-7** were obtained for the hydrochloride salts and the neat free base form and are supplied as Supporting Information (Figure S 47-57) with an enlarged fingerprint region and annotation for facile identification. In addition, spectra of the free bases obtained from GC-solid state IR analysis of compounds **3, 4, 5** and **7** are also provided (Figure S 58-65). All spectra were dominated by the C=O absorptions in a narrow range of 1716-1742 for the salts and 1723-1732 cm^{-1} for the free bases, respectively. A summary of the most distinct bands is given in Table 4, which can be used for structure confirmation.

Conclusion

The Internet and dark web have been strong drivers for the distribution of psychoactive substances in the last decade, with NPS being marketed at an ever increasing pace. Herein, the structural and spectral properties of six phenidate analogs were determined by employing a combination of X-ray crystallography, NMR spectroscopy, GC-MS, QTOF-MS/MS, IR spectroscopy and DFT computations. These analytical data can be used for future structural elucidation of novel phenidate analogs and provide support to analytical data interpretation. Thermal decomposition of phenidate analogs under GC-MS standard conditions served as a reminder of the challenges encountered within the field of forensic chemistry. The observed thermal decomposition might also be a phenomenon linked to vaporizing as a form of drug administration (consumption) which might yield similar degradation products.

Acknowledgments

We thank Dr. Nils Schlörer and Kerstin König (both University of Cologne) for swift NMR measurements. SDB thanks Isomer Design (Toronto, Canada) for support.

References

- [1] Council of the European Union. Council Decision 2005/387/JHA of 10 May 2005 on the information exchange, risk-assessment and control of new psychoactive substances. *Off. J. European Union*. **2005**. L127, 32.
- [2] S.D. Brandt, L.A. King, M. Evans-Brown. The new drug phenomenon. *Drug. Test. Anal.* **2014**, 6, 587.
- [3] European Monitoring Centre for Drugs and Drug Addiction, *European Drug Report 2016: Trends and Developments*. Publications Office of the European Union, Luxembourg, **2016**. Available at: <http://www.emcdda.europa.eu/system/files/publications/2637/TDAT16001ENN.pdf> [20 August 2016]
- [4] European Monitoring Centre for Drugs and Drug Addiction – *Europol*. *EMCDDA-Europol 2015 Annual Report on the implementation of Council Decision 2005/387/JHA*. Publications Office of the European Union, Luxembourg, **2016**. Available at: <http://www.emcdda.europa.eu/system/files/publications/2880/TDAS16001ENN.pdf> [20 August 2016]
- [5] European Monitoring Centre for Drugs and Drug Addiction, *The internet and drug markets*. Publications Office of the European Union, Luxembourg, **2016**. Available at: http://www.emcdda.europa.eu/system/files/publications/2155/TDXD16001ENN_FINAL.pdf [20 August 2016]
- [6] J.M. Axten, L. Krim, H.F. Kung, J.D. Winkler. A stereoselective synthesis of dl-threo-methylphenidate: preparation and biological evaluation of novel analogs. *J. Org. Chem.* **1998**, 63, 9628.
- [7] S.J. Gatley, D. Pan, R. Chen, G. Chaturvedi, Y.S. Ding. Affinities of methylphenidate derivatives for dopamine, norepinephrine and serotonin transporters. *Life Sci.* **1996**, 58, 231.

- [8] D.I. Kim, H.M. Deutsch, X. Ye, M.M. Schweri. Synthesis and pharmacology of site-specific cocaine abuse treatment agents: restricted rotation analogs of methylphenidate. *J. Med. Chem.* **2007**, *50*, 2718.
- [9] M. Steele, M. Weiss, J. Swanson, J. Wang, R.S. Prinzo, C.E. Binder. A randomized, controlled effectiveness trial of OROS-methylphenidate compared to usual care with immediate-release methylphenidate in attention deficit-hyperactivity disorder. *Can. J. Clin. Pharmacol.* **2006**, *13*, e50.
- [10] R.C. Spencer, D.M. Devilbiss, C.W. Berridge. The cognition-enhancing effects of psychostimulants involve direct action in the prefrontal cortex. *Biol. Psychiatry* **2015**, *77*, 940.
- [11] W. Klein-Schwartz. Abuse and toxicity of methylphenidate. *Curr. Opin. Pediatr.* **2002**, *14*, 219.
- [12] C. Bissig. Neuro-Enhancement und neue psychoaktive Substanzen (NPS) *NPS-News*, **2015**, *3*, starting page.
- [13] J. Spensley, D.A. Rockwell. Psychosis during methylphenidate abuse. *New Engl. J. Med.* **1972**, *286*, 880.
- [14] S. Beharry, S. Gibbons. An overview of emerging and new psychoactive substances in the United Kingdom. *Forensic Sci. Int.* **2016**, *267*, 25.
- [15] G. McLaughlin, N. Morris, P. V. Kavanagh, J. D. Power, G. Dowling, B. Twamley, J. O'Brien, G. Hessman, B. Murphy, D. Walther, J. S. Partilla, M. H. Baumann, S. D. Brandt. Analytical characterization and pharmacological evaluation of the new psychoactive substance 4-fluoromethylphenidate (4F-MPH) and differentiation between the (±)-threo- and (±)-erythro diastereomers. *Drug Test. Anal.* **2017**, doi: XXX

- [16] M. Misra, Q. Shi, X.C. Ye, E. Gruszecka-Kowalik, W. Bu, Z.Z. Liu, M.M. Schweri, H.M. Deutsch, C.A. Venanzi. Quantitative structure-activity relationship studies of threo-methylphenidate analogs. *Bioorg. Med. Chem.* **2010**, *18*, 7221.
- [17] L. D. Simmler, D. Buchy, S. Chaboz, M. C. Hoener, M. E. Liechi. In vitro characterization of psychoactive substances at rat, mouse, and human trace amine-associated receptor. *J. Pharmacol. Exp. Ther.* **2016**, *357*, 134.
- [18] M. R. Meyer, A. Schütz, H. H. Maurer. Contribution of human esterases to the metabolism of selected drugs of abuse. *Toxicol. Lett.* **2015**, *232*, 159.
- [19] G.P. Bailey, J.H. Ho, S. Hudson, A. Dines, J.R. Archer, P.I. Dargan, D.M. Wood. Nopaine no gain: recreational ethylphenidate toxicity. *Clin. Toxicol.* **2015**, *53*, 498.
- [20] C. Parks, D. McKeown, H.J. Torrance. A review of ethylphenidate in deaths in east and west Scotland. *Forensic Sci. Int.* **2015**, *257*, 203.
- [21] P.D. Maskell, P.R. Smith, R. Cole, L. Hikin, S.R. Morley. Seven fatalities associated with ethylphenidate. *Forensic Sci. Int.* **2016**, *265*, 70.
- [22] C. Lafferty, L. Smith, A. Coull, J. Shanley. The experience of an increase in the injection of ethylphenidate in Lothian April 2014-March 2015. *Scott. Med. J.* **2016**, DOI: 10.1177/0036933016649871
- [23] J. Krueger, H. Sachs, F. Musshoff, T. Dame, J. Schaeper, M. Schwerer, M. Graw, G. Roeder. First detection of ethylphenidate in human fatalities after ethylphenidate intake. *Forensic Sci. Int.* **2014**, *243*, 126.
- [24] K.S. Patrick, R.L. Williard, A.L. VanWert, J.J. Dowd, J.E. Oatis, Jr., L.D. Middaugh. Synthesis and pharmacology of ethylphenidate enantiomers: the human transesterification metabolite of methylphenidate and ethanol. *J. Med. Chem.* **2005**, *48*, 2876.

- [25] J.S. Markowitz, C.L. Devane, D.W. Boulton, Z. Nahas, S.C. Risch, F. Diamond, K.S. Patrick. Ethylphenidate formation in human subjects after the administration of a single dose of methylphenidate and ethanol. *Drug Metab. Dispos.* **2000**, 28, 620.
- [26] R. Williard, L. Middaugh, H-J. Zhu, K. S. Patrick. Methylphenidate and its ethanol transesterification metabolite ethylphenidate: brain disposition, monoamine transporters and motor activity. *Behav. Pharmacol.* **2007**, 18(1), 39.
- [27] European Monitoring Centre for Drugs and Drug Addiction. New psychoactive substances in Europe: Innovative legal responses. Publications Office of the European Union, Luxembourg. **2015**. Available at: <http://www.emcdda.europa.eu/system/files/publications/975/TD0215501ENN.pdf> [20 August 2016]
- [28] European Court of Justice. Mixtures of herbs containing synthetic cannabinoids consumed as a marijuana substitute are not medicinal products, 10.07.2014, C-358/13, C-181/14. Available at: http://insolvency-law7.eu/master.php?wahl=31&u_id=155973 [20 August 2016]
- [29] Gesetz zur Bekämpfung der Verbreitung neuer psychoaktiver Stoffe. **2016**, *Bundesgesetzblatt*, **2016**, 1, 55, 2615
- [30] Cambridge Crystallographic Data Centre. Available at: http://www.ccdc.cam.ac.uk/data_request/cif.
- [31] R. Ahlrichs, M. Bär, M. Häser, H. Horn, C. Kölmel. Electronic-structure calculations on workstation computers: the program system Turbomole. *Chem. Phys. Lett.* **1989**, 162, 165.
- [32] A. Schäfer, H. Horn, R. Ahlrichs. Fully Optimized Contracted Gaussian-Basis Sets for Atoms Li to Kr. *J. Chem. Phys.* **1992**, 97, 2571.

- [33] F. Weigend, R. Ahlrichs. Balanced basis sets of split valence, triple zeta valence and quadruple zeta valence quality for H to Rn: Design and assessment of accuracy. *Phys. Chem. Chem. Phys.* **2005**, *7*, 3297.
- [34] P.J. Stephens, F.J. Devlin, C.S. Ashvar, C.F. Chabalowski, M.J. Frisch. Theoretical Calculation of Vibrational Circular-Dichroism Spectra. *Faraday Discuss.* **1994**, *99*, 103.
- [35] S. Grimme, J. Antony, S. Ehrlich, H. Krieg. A consistent and accurate ab initio parametrization of density functional dispersion correction (DFT-D) for the 94 elements H-Pu. *J. Chem. Phys.* **2010**, *132*,
- [36] S. Grimme, S. Ehrlich, L. Goerigk. Effect of the damping function in dispersion corrected density functional theory. *J. Comput. Chem.* **2011**, *32*, 1456.
- [37] M. Froimowitz, K.-M. Wu, C. George, D. VanDerveer, Q. Shi, H.M. Deutsch. Crystal structures of analogs of threo-methylphenidate. *Struct. Chem.* **1998**, *9*, 295.
- [38] M.M. Schweri, H.M. Deutsch, A.T. Massey, S.G. Holtzman. Biochemical and behavioral characterization of novel methylphenidate analogs. *J. Pharmacol. Exp. Ther.* **2002**, *301*, 527
- [39] N. Uchiyama, S. Matsuda, M. Kawamura, Y. Shimokawa, R. Kikura-Hanajiri, K. Aritake, Y. Urade, Y. Goda. Characterization of four new designer drugs, 5-chloro-NNEI, NNEI indazole analog, α -PHPP and α -POP, with 11 newly distributed designer drugs in illegal products. *Forensic. Sci. Int.* **2014**, *243*, 1.
- [40] J. F. Casale, P. A. Hays. Ethylphenidate: an analytical profile. *Microgram J.* **2011**, *8*, 58.
- [41] B. L. Flamm, J. Gal. The thermal decomposition of methylphenidate in the gas chromatograph mass spectrometer. *Biomed. Mass. Spectrom.* **1975**, *2*, 281.
- [42] K. Tsujikawa, Y. T. Iwata, M. Inoue, S. Higashibayashi, H. Inoue. Comments on "Characterization of four new designer drugs, 5-chloro-NNEI, NNEI indazole analog, α -

PHPP and α -POP, with 11 newly distributed designer drugs in illegal products". *Forensic Sci. Int.* **2015**, 251, e15-e17.

[43] K. Sujatha, T. Arundathi, S. Rubina, B. V. Ramana, G. Nagarajan. Drug delivery methods ranking addiction potential. *Int. J. Pharm. Sci. Res.* **2013**, 4, 1287.

[44] UK Chemical Research. Converting RCs to freebase, <https://www.ukchemicalresearch.org/User-freakiestgolf> (2013, June, 20). Available at: <https://www.ukchemicalresearch.org/Thread-Converting-RCs-to-freebase> [20 August 2016]

[45] C. Soussan, A. Kjellgren. "Chasing the high" – experiences of ethylphenidate as described on international internet forums. *Subst. Abuse* **2015**, 9, 9.

[46] N. Negreira, C. Erratico, A.L.N. van Nuijs, A. Covaci. Identification of in vitro metabolites of ethylphenidate by liquid chromatography coupled to quadrupole time-of-flight mass spectrometry. *Forensic Sci. Int.* **2016**, 117, 474.

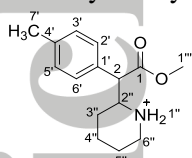
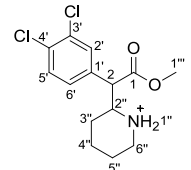
Accepted Article

Table 1: Dihedral angles and geometric distances in crystal structures **2-7** and computed minimum energy geometry for **7**.

	2	3	4	5 ^[a]	6	7 ^[b]
C2'-C1'-C2-C3 (°)	72	72	64	44, 58	82	69 [59]
N1-C3-C2-C1 (°)	-56	-73	-65	-64, -70	-73	-64 [-59]
C3-C2-C1-O1 (°)	143	-39	-32	-43, -34	-36	164 [147]
N1-O1 (Å)	3.78	3.46	3.21	3.34, 3.34	3.38	4.08 [3.94]
N1-O2 (Å)	3.14	3.90	3.90	3.74, 3.87	3.84	3.02 [3.20]

[a] Two symmetrically independent molecules in crystal structure. [b] Computed values in parantheses, BP86-D3(BJ)/def2-TZVP in gas phase (*ax-7-1*).

Table 2: NMR assignments of compounds **2** to **7** as their salts, α and β denominate diastereotopic protons with α being the one shifted further downfield

4-Methylmethylphenidate 2 HCl (300 MHz, CDCl ₃ , 298 K)		
		
No.	¹³ C [δ / ppm]	¹ H [δ / ppm]
1	172.18	-
2	53.71	4.26 (d, <i>J</i> = 10.3 Hz, 1H)
1'	131.13	-
2', 6'	128.29	7.20 – 7.08 (m, 4H) ^a
3', 5'	129.98	7.20 – 7.08 (m, 4H) ^a
4'	138.34	-
7'	21.20	2.31 (s, 3H)
1''	-	10.24 ((d), <i>J</i> = 10.6 Hz, NH, 1H) 8.93 ((d), <i>J</i> = 11.9 Hz, NH', 1H)
2''	59.09	3.72 – 3.58 (m, 2H) ^b
3''	25.96	1.73 – 1.58 (m, H-3'' α , 1H) 1.43 – 1.23 (m, H-3'' β , 2H) ^c
4''	22.65	1.87 – 1.74 (m, H-4'' α , 2H) ^d 1.43 – 1.23 (m, H-4'' β , 2H) ^c
5''	22.03	2.15 – 1.96 (m, H-5'' α , 1H) 1.87 – 1.74 (m, H-5'' β , 2H) ^d
6''	45.66	3.72 – 3.58 (m, H-6'' α , 2H) ^b 2.90 (m, H-6'' β , 1H)
1'''	53.42	3.79 (s, 3H)
^a Protons H-2'/6' and H-3'/4 H' overlap ^b Protons H-2'' and H-6'' α overlap ^c Protons H-3'' β and H-4'' β overlap ^d Protons H-4'' α and H-5'' β overlap		
		
3,4-Dichloromethylphenidate 3 HCl (300 MHz, 298 K, CDCl ₃ + MeOD)		
No.	¹³ C [δ / ppm]	¹ H [δ / ppm]
1	171.66	-
2	52.79	4.30 (d, <i>J</i> = 10.1 Hz, 1H)
1'	133.04	-
2'	130.37	7.37 (d, <i>J</i> = 2.1 Hz, 1H)
3'	133.54	-
4'	134.01	-
5'	131.31	7.42 (d, <i>J</i> = 8.3 Hz, 1H)
6'	128.09	7.12 (dd, <i>J</i> = 8.3, 2.2 Hz, 1H)
1''	-	^a
2''	58.50	3.66 – 3.48 (m, 2H) ^b
3''	25.89	1.72 – 1.59 (m, H-3'' α , 1H) 1.46 – 1.27 (m, H-3'' β , 2H) ^c
4''	22.48	1.85 – 1.80 (m, H-4'' α , 2H) ^d

5''	21.86	1.46 – 1.27 (m, H-4''β, 2H) ^c 2.07 – 1.89 (m, H-5''α, 1H) 1.85 – 1.80 (m, H-5''β, 2H) ^d
6''	45.77	3.66 – 3.48 (m, H-6''α, 2H) ^b 2.89 ((td), <i>J</i> = 12.8, 3.3 Hz, 1H)
1'''	53.52	3.74 (s, 3H)

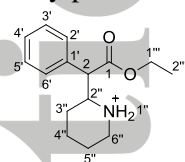
^aNH/NH' not observed

^bProtons H-2'' and H-6''α overlap

^cProtons H-3''β and H-4''β overlap

^dProtons H-4''α and H-5''β overlap

Ethylphenidate **4** HCl (300 MHz, 298 K, CDCl₃)



No.	¹³ C [δ / ppm]	¹ H [δ / ppm]
1	171.76	-
2	54.11	4.34 – 4.10 (m, 3H) ^b
1'	134.32	-
2', 6'	128.55	7.37 – 7.14 (m, 5H) ^a
3', 5'	129.29	7.37 – 7.14 (m, 5H) ^a
4'	128.43	7.37 – 7.14 (m, 5H) ^a
1''	-	10.36 (s, NH, 1H) 8.68 (s, NH', 1H)
2''	59.10	3.68 – 3.56 (m, 2H) ^c
3''	25.94	1.77 – 1.61 (m, H-3''α, 3H) ^d 1.35 – 1.26 (m, H-3''β, 2H) ^e
4''	22.64	1.77 – 1.61 (m, H-4''α, 3H) ^d 1.35 – 1.26 (m, H-3''β, 2H) ^e
5''	21.99	2.05 – 1.96 (m, 1H, H-5''α) 1.77 – 1.61 (m, H-5''β, 3H) ^d
6''	45.74	3.68 – 3.56 (m, H-6''α, 2H) ^c 2.86 (t, <i>J</i> = 12.8 Hz, 1 H)
1'''	62.51	4.34 – 4.10 (m, H-1'''α, 3H) ^b 4.34 – 4.10 (m, H-1'''β, 3H) ^b
2'''	13.97	1.13 ((t), <i>J</i> = 7.1 Hz, 3H)

^aProtons H-2', H-3', H-4', H-5' and H-6' overlap

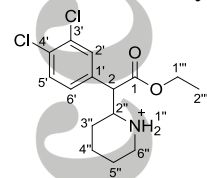
^bProtons H-2, H-1'''α and H-1'''β overlap

^cProtons H-2'' and H-6''α overlap

^dProtons H-3''α, H-4''α and H-5''β overlap

^eProtons H-3''β and H-4''β overlap

3,4-Dichloroethylphenidate **5** (300 MHz, 298 K, CDCl₃)



No.	¹³ C [δ / ppm]	¹ H [δ / ppm]
1	170.63	-
2	53.26	4.38 – 4.20 (m, 3H) ^b
1'	132.92	-
2'	130.51	7.45 – 7.38 (m, 2H) ^a
3'	133.47	-
4'	134.30	-

5'	131.23	7.45 – 7.38 (m, 2H) ^a
6'	128.03	7.15 (dd, 8.3, 2.1 Hz, 1H)
1''	-	10.19 (m, NH, 1H)
2''	58.66	9.07 (m, NH', 1H)
3''	25.98	3.72 – 3.60 (m, 2H) ^c
4''	22.59	1.75 – 1.62 (m, H-3'' α , 1H)
5''	21.97	1.50 – 1.30 (m, H-3'' β , 2H) ^d
6''	45.73	1.84 – 1.78 (m, H-4'' α , 2H) ^e
1'''	62.89	2.05 – 1.96 (m, H-5'' α , 1H)
2'''	13.97	1.84 – 1.78 (m, H-5'' β , 2H) ^e
		3.72 – 3.60 (m, H-6'' α , 2H) ^c
		2.90 ((q), $J = 11.8$ Hz, 1H)
		4.38 – 4.20 (m, H-2''' α/β , 3H) ^b
		1.21 ((t), $J = 7.1$ Hz, 3H)

^aProtons H-2' and H-5' overlap

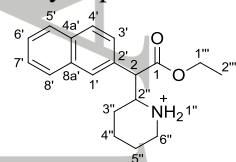
^bProtons H-2 and H-2''' α/β overlap

^cProtons H-2'' and H-6'' α overlap

^dProtons H-3'' β and H-4'' β overlap

^eProtons H-4'' α and H-5'' β overlap

Ethyl-naphthidate **6** CH₃SO₃H (300 MHz, 298 K, CDCl₃)



No.	¹³ C [δ / ppm]	¹ H [δ / ppm]
1	171.93	-
2	53.85	4.38 (d, $J = 9.9$ Hz, 1 H)
1'	128.37	7.90 – 7.69 (m, 4H) ^a
2'	131.69	-
3'	125.67	7.37 (dd, $J = 8.6, 1.8$ Hz, 1H)
4'	128.11	7.90 – 7.69 (m, 4H) ^a
4a'	133.03	-
5'	129.11	7.90 – 7.69 (m, 4H) ^a
6'	126.58	7.57 – 7.42 (m, 2H) ^b
7'	126.67	7.57 – 7.42 (m, 2H) ^b
8'	127.78	7.90 – 7.69 (m, 4H) ^a
8a'	133.51	-
1''	-	9.01 (m, NH, 1H)
		8.38 (m, NH', 1H)
2''	58.79	3.87 – 3.62 (m, 2H) ^d
3''	26.17	1.71 – 1.58 (m, H-3'' α , 1H)
4''	22.54	1.48 – 1.24 (m, H-3'' β , 2H) ^c
5''	22.13	2.00 – 1.71 (m, H-4'' α , 3H) ^f
6''	46.28	1.48 – 1.24 (m, H-4'' β , 2H) ^c
		2.00 – 1.71 (m, H-5'' α , 3H) ^f
		2.00 – 1.71 (m, H-5'' β , 3H) ^f
		3.87 – 3.62 (m, H-6'' α , 2H) ^d
		3.04 ((q), $J = 12.0, 11.6$ Hz, H-6'' β , 1H)
1'''	62.13	4.23 (m, 2H) ^c
2'''	13.94	1.15 ((t), $J = 7.1$ Hz, 3H)

^aProtons H-1', H-4', H-5' and H-8' overlap

^bProtons H-6' and H-7' overlap

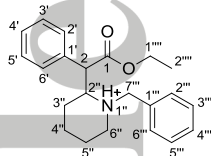
^cProtons H-1'' α and H-1'' β overlap

^dProtons H-2'' and H-6'' α overlap

^aProtons H-3''β and H-4''β overlap

^bProtons H-4''α, H-5''α and H-5''β overlap

N-Benzyl-ethylphenidate **7** HCl (600 MHz, 298 K, CDCl₃)



No.	¹³ C [δ / ppm]	¹ H [δ / ppm]
1	170.63	-
2	52.21	5.02 (d, <i>J</i> = 8.3 Hz, 1H)
1'	134.62	-
2', 6'	129.18	7.39 – 7.30 (m, 3H) ^a
3', 5'	129.27	7.53 – 7.39 (m, 5 H) ^b
4'	128.35	7.39 – 7.30 (m, 3H) ^a
1''	-	12.48 (s, NH, 1H)
2''	67.01	3.97 (ddt, <i>J</i> = 12.6, 8.3, 4.0 Hz, 1H)
3''	27.50	2.14 – 1.93 (m, H-3''α, 2H) ^c 1.25 – 1.18 (m, H-3''β, 1H)
4''	22.83	1.86 – 1.61 (m, H-4''α, 2H) ^d 1.43 – 1.27 (m, H-4''β, 1H)
5''	22.41	2.14 – 1.93 (m, H-5''α, 2H) ^c 1.86 – 1.61 (m, H-5''β, 2H) ^d
6''	52.48	3.30 – 3.14 (m, H-6''α, 1H) 2.51 (tdd, <i>J</i> = 12.4, 9.3, 3.0 Hz, H-6''β, 1H)
1'''	129.34 ^e	-
2''' , 6'''	131.57	7.87 – 7.78 (m, 2H)
3''' , 5'''	129.49	7.53 – 7.39 (m, 5 H) ^b
4'''	130.01	7.53 – 7.39 (m, 5 H) ^b
7'''	57.49	4.72 (dd, <i>J</i> = 12.2, 3.6 Hz, H-7'''α, 1H) 3.68 (dd, <i>J</i> = 12.3, 8.7 Hz, H-7'''β, 1H)
1''''	62.24	4.31 – 4.06 (m, H-1''''α/β, 2H)
2''''	13.85	1.14 ((t), <i>J</i> = 7.1 Hz, 3H)

^aProtons H-2'/6' and H-4' overlap

^bProtons H-3'/5', H-3'''/5''' and H-4''' overlap

^cProtons H-3''α and H-5''α overlap

^dProtons H-4''α and H-5''β overlap

^eAssigned through correlation, very weak

Table 3: Molecular ions (MS-TOF) and product ions (MS/MS-TOF) with formulas for compounds **2-7** from pathways **A-C**, **D** denotes significant other fragments. Deviations are given in parentheses.

Compound	[M+H] ppm)	(Δ [A+H] ppm)	(Δ [B+H] (Δ ppm)	[C+H] ppm)	(Δ D (Δ ppm)
2	248.1646 (-2.5) C ₁₅ H ₂₂ NO ₂	-	188.1436 (-1.0) C ₁₃ H ₁₈ N	84.081 (6.0) C ₅ H ₁₀ N	-
3	302.0716 (-2.1) C ₁₄ H ₁₈ Cl ₂ NO ₂	-	242.0498 (-0.3) C ₁₂ H ₁₄ Cl ₂ N	84.0811 (-3.4) C ₅ H ₁₀ N	-
4	248.1655 (-3.8) C ₁₅ H ₂₂ NO ₂	220.1336 (2.0) C ₁₃ H ₁₈ NO ₂	174.1277 (-1.2) C ₁₂ H ₁₆ N	84.0813 (6.7) C ₅ H ₁₀ N	-
5	316.0869 (-1.1) C ₁₅ H ₂₀ Cl ₂ NO ₂	288.0550 (1.3) C ₁₃ H ₁₆ Cl ₂ NO ₂	242.0499 (0.0) C ₁₂ H ₁₄ Cl ₂ N	84.0810 (2.6) C ₅ H ₁₀ N	-
6	298.1807 (-1.8) C ₁₉ H ₂₄ NO ₂	270.1493 (-1.5) C ₁₇ H ₂₀ NO ₂	224.1442 (-3.7) C ₁₆ H ₁₈ N	84.0807 (0.9) C ₅ H ₁₀ N	141.0704 (-3.5) C ₁₁ H ₉
7	338.2109 (1.5) C ₂₂ H ₂₈ NO ₂	310.1807 (3.4) C ₂₀ H ₂₄ NO ₂	174.1277 (-7.2) C ₁₂ H ₁₆ N	174.1277 (-7.2) C ₁₂ H ₁₆ N	246.1493 (-1.7) C ₁₅ H ₂₀ NO ₂

Table 4: Experimental wavenumbers (cm⁻¹) for phenidate analogs 2-7.^[a]

	2	3	4	5	6	7
ν C=O ^[b]	1730 (s)	1732 (s)	1724 (s)	1727 (s)	1723 (s)	1732 (s)
ν N-H (valence)	3507 (w)	n. o.				
ν C _{al} -H (valence)	2858 (w)	2710 (m)	2854 (m)	2707 (s)	2653 (m)	2634 (w)
ν C=O (valence)	1716 (m)	1735 (s)	1721 (m)	1729 (s)	1723 (w)	1742 (m)
ν C-O-R (valence)	1187 (s)	1137 (s)	1173 (s)	1208 (m)	1272 (w)	1230 (s)
	1024 (s)	932 (m)	1024 (s)	1178 (s)	749 (m)	733 (s)
Fingerprint	760 (s)	673 (m)	744 (s)	1026 (s)	604 (w)	608 (s)
	483 (s)	441 (s)	704 (s)	449 (m)	507 (m)	507 (s)

[a] (w) = weak, (m) = medium, (s) = strong, n. o. = not observed. [b] Free base.

Accepted Article

NPS Distribution 2012-2015 at Customs Cologne

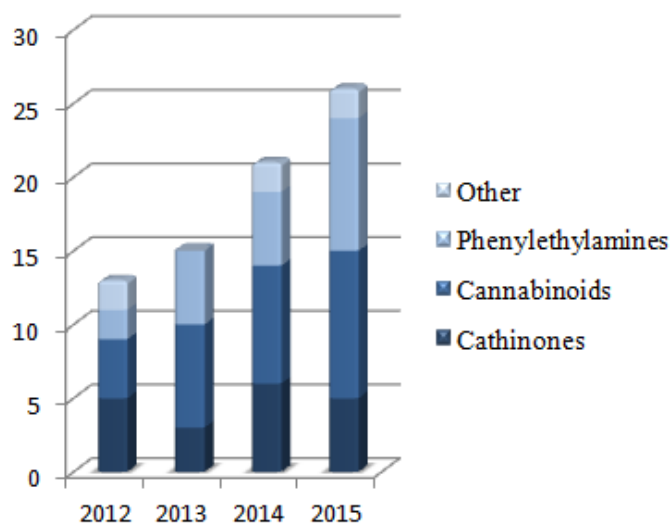
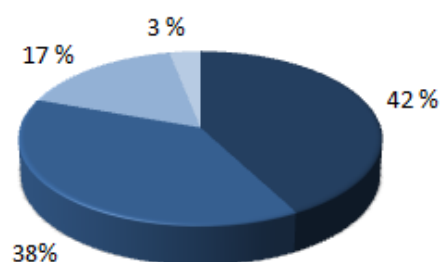


Figure 1: Distribution of NPS cases by substance-class (legal and illegal combined) and total amount of identified substances not listed under the German Narcotics Act in the years 2012-2015 at the Centre of Education and Science of the Central Customs Authority Cologne

Accepted

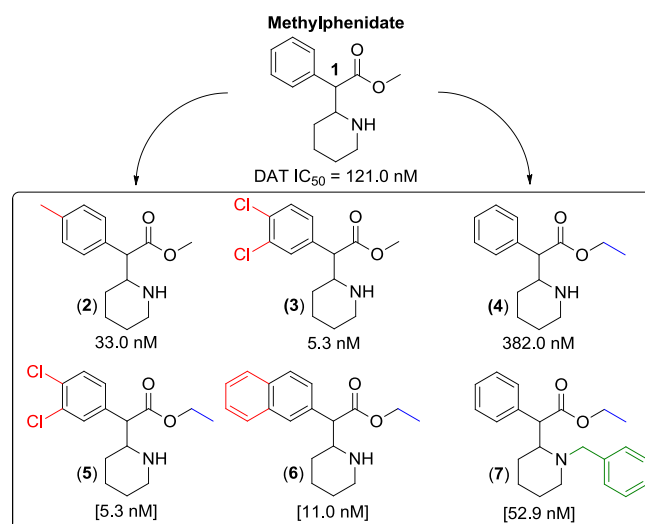


Figure 2: Analyzed NPS derived from *threo*-methylphenidate, alterations at the aryl-moiety (red), the ester group (blue) and substitution at nitrogen (green) with their DAT IC₅₀ values. Numbers in parentheses correspond to the values for the known parent methyl-ester compounds.^[15,25]

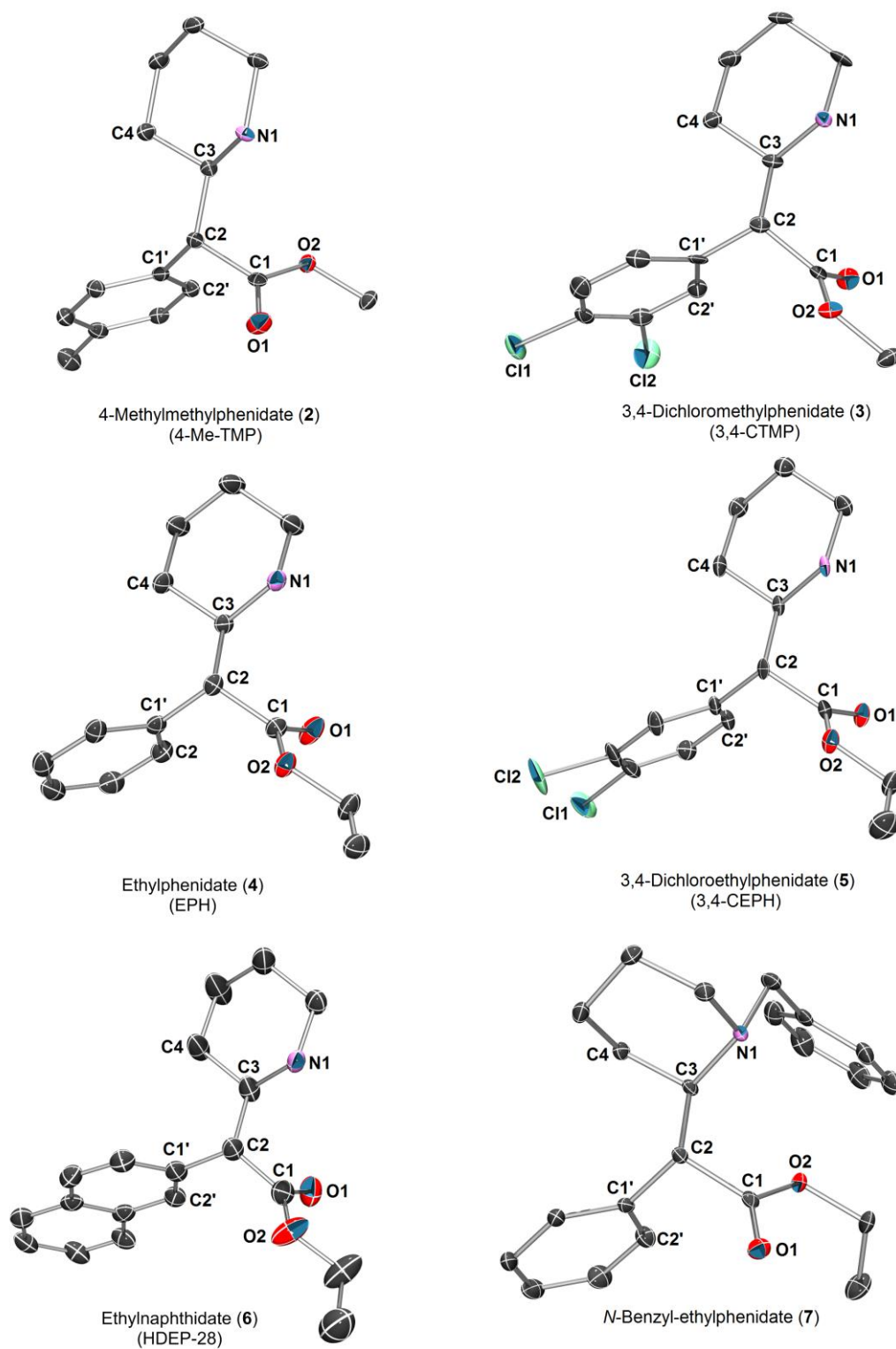


Figure 3: X-ray crystal structures of phenidate analogs (\pm)-*threo*-2-7 HCl with thermal ellipsoids at the 50% probability level, depicted in (*R,R*)-configuration with their common abbreviations in parentheses. Hydrogen atoms have been omitted for clarity.

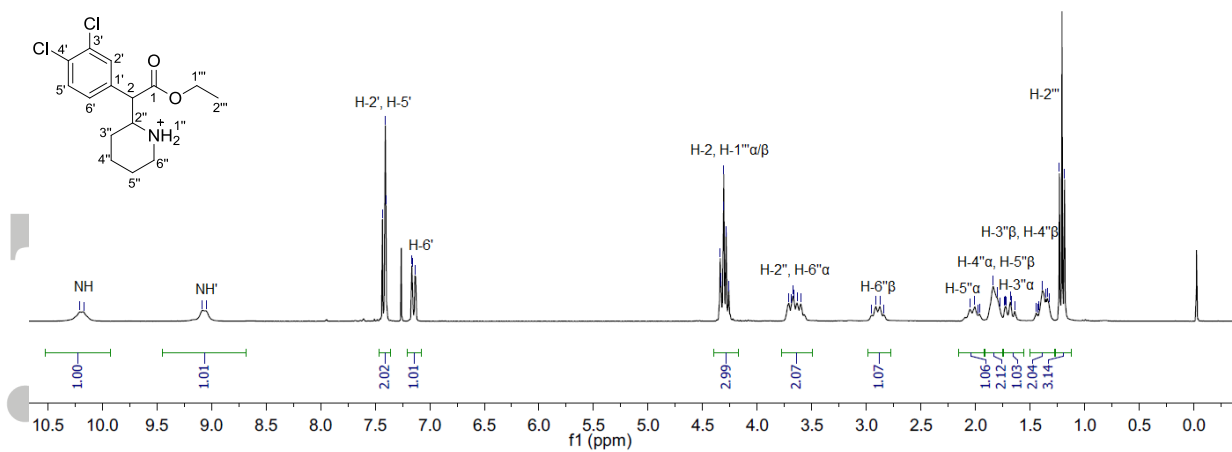


Figure 4: $^1\text{H-NMR}$ of 3,4-dichloroethylphenidate **5** with assignments (300 MHz, 298 K, CDCl_3), α and β denote diastereotopic protons where α was the one shifted further downfield.

Accepted Article

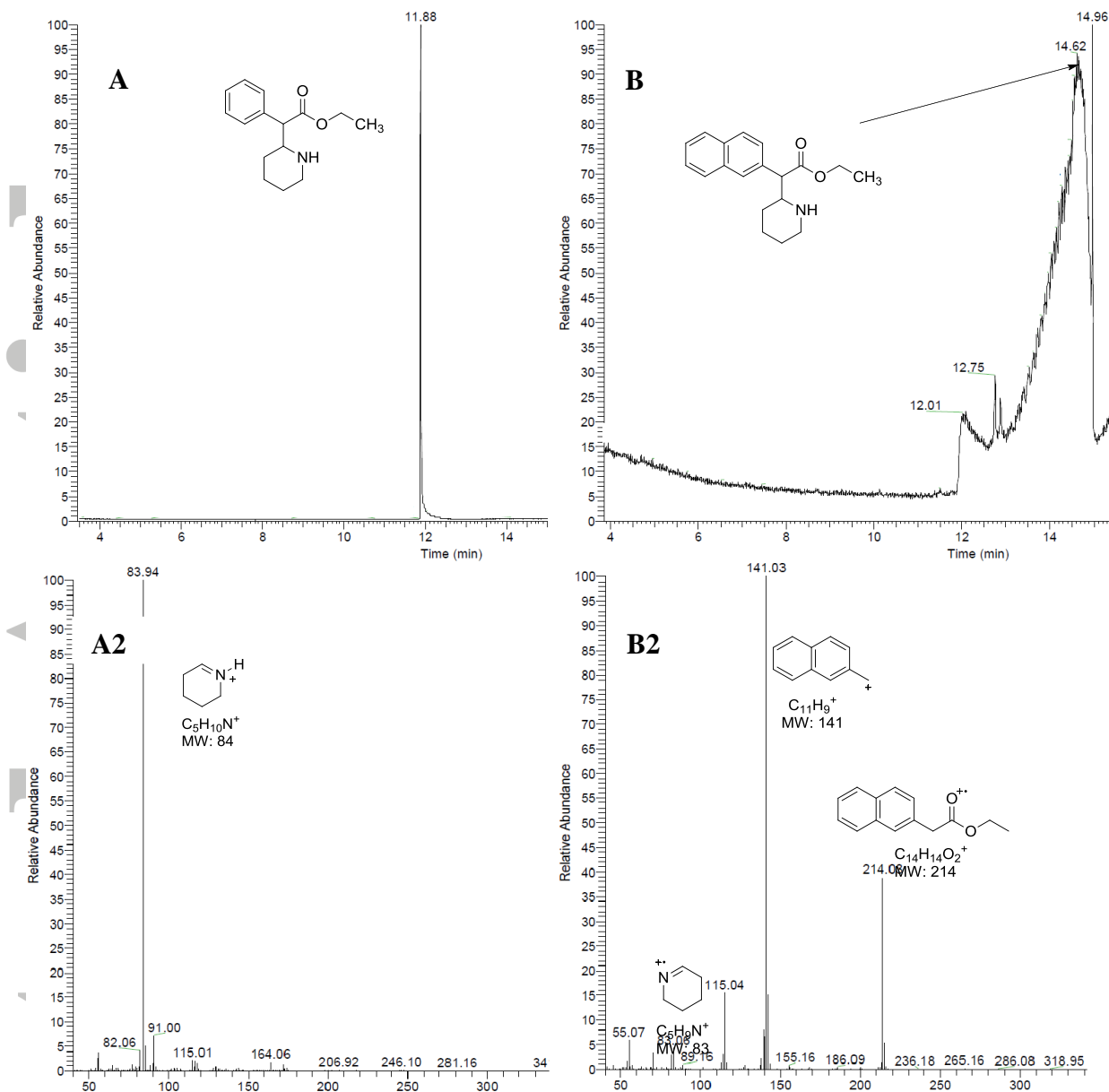


Figure 5: GC-chromatograms of ethylphenidate **4** (A) and ethylnaphthidate **6** (B) (top). Compound **4** showed little signs of thermal decomposition under standard GC-conditions, while **6** decomposed to 2-naphthyl-ethylacetate and 2,3,4,5-tetrahydropyridine. EI-MS spectra (bottom) of ethylphenidate **4** (A2) at 11.88 min and the thermal decomposition products of ethylnaphthidate **6** (B2) at 14.63 min (major peak in GC).

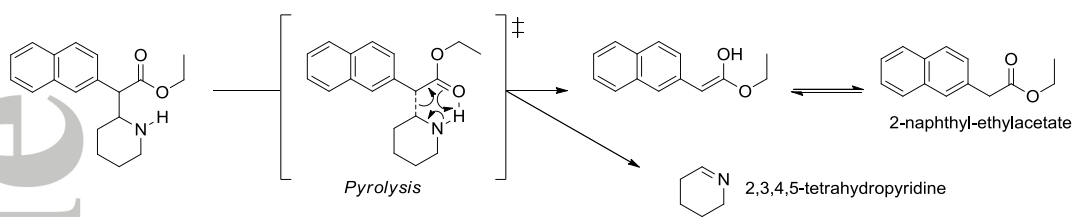


Figure 6: Proposed pyrolysis of ethylnaphthidate **6** in the injection port and/or on column under standard GC-conditions. Analogous thermal decomposition predominantly occurs with compounds **3** and **5**.

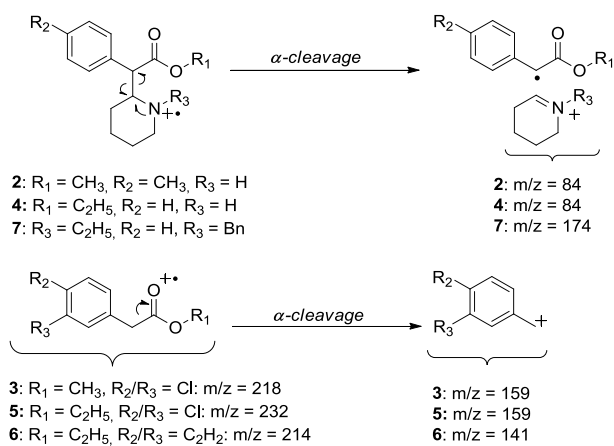


Figure 7: Main fragments observed in the EI-mass spectra of the major peaks in GC of compounds **2-7**.

Compounds **3, 5** and **6** thermally decompose on GC to their corresponding 2-aryl-acetates.

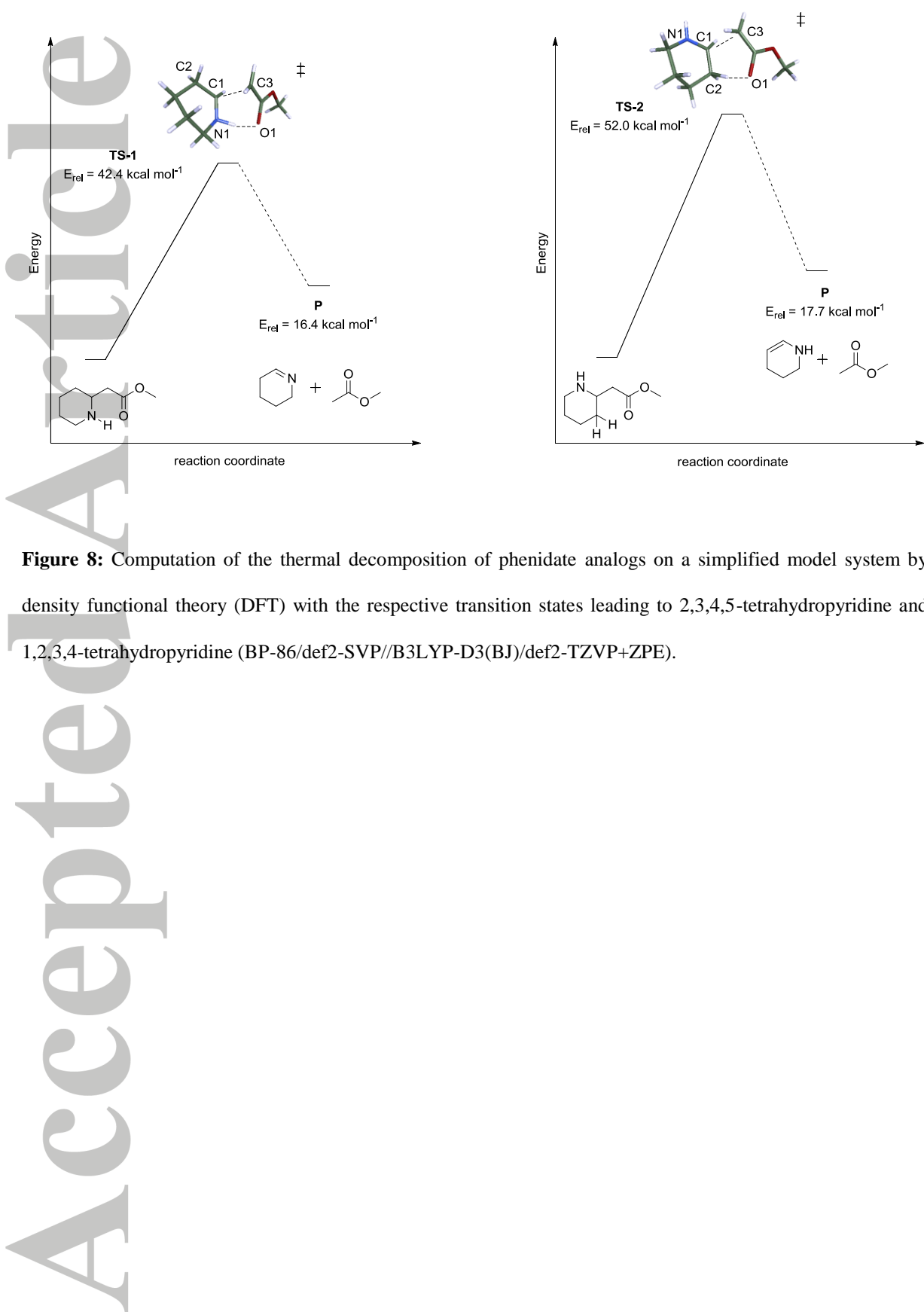


Figure 8: Computation of the thermal decomposition of phenidate analogs on a simplified model system by density functional theory (DFT) with the respective transition states leading to 2,3,4,5-tetrahydropyridine and 1,2,3,4-tetrahydropyridine (BP-86/def2-SVP//B3LYP-D3(BJ)/def2-TZVP+ZPE).

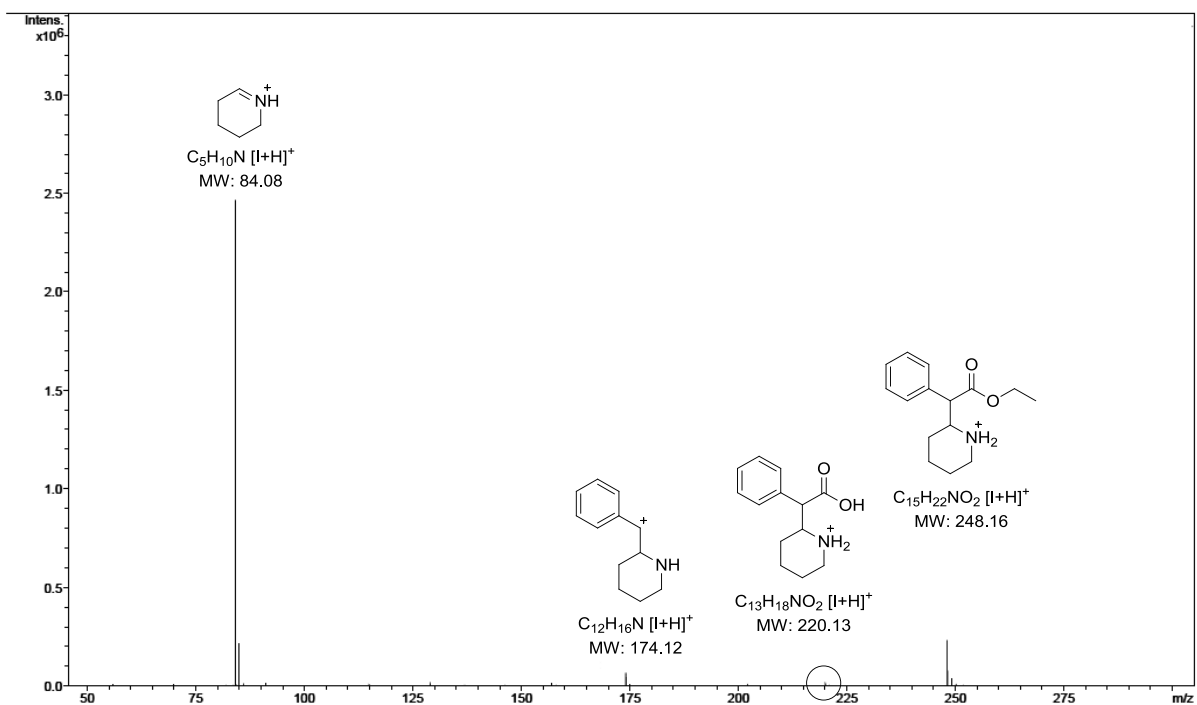


Figure 9: Product ion spectrum of ethylphenidate **4** (CE = 26.0 eV), the signal for the fragmentation pathway **A** (Figure 10) has a very low intensity.

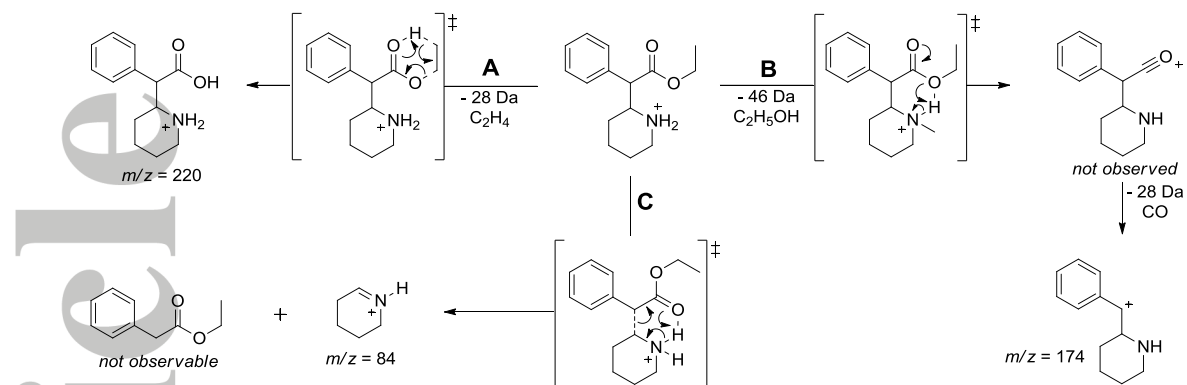
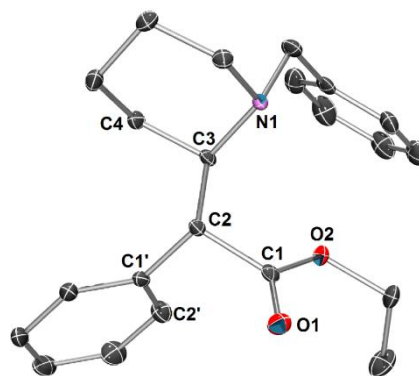


Figure 10: Proposed fragmentation pathways A-C of ethylphenidate 4 under ESI-MS/MS conditions. Product ion formation was similar for all derivatives 2-7 depending on their molecular structure but pathway A cannot occur for methylphenidates 2 and 3.

Table of Contents

Six analogs of methylphenidate (Ritalin®) were analyzed and fully characterized by X-ray, NMR, GC-EI-MS, ESI-MS² and FT-IR. Thermal decomposition of phenidates on column under routine GC-MS conditions was rationalized by experiment and DFT-computations.



Analysis of six “neuro-enhancing” phenidate analogs

Helge Klare, Jörg M. Neudörfl, Simon D. Brandt, Elisabeth Mischler, Sigrid Meier-Giebing,
Kathrin Deluweit, Folker Westphal, Tim Laussmann *